

Evidence for Electron Correlation in the Two-Electron Continuum during Double Ionization in 300-keV $H^+ + He$ Collisions

B. Skogvall^(a) and G. Schiwietz

Department P3, Hahn-Meitner-Institut Berlin GmbH, Glienicker Strasse 100, D-1000 Berlin 39, Federal Republic of Germany
(Received 30 April 1990)

Absolute differential ionization probabilities for small-impact-parameter $H^+ + He$ collisions were measured as a function of the electron energy, electron ejection angle, and final recoil-ion charge state. Good agreement was found between the experimental angular distribution of ejected electrons and results of a coupled-channel calculation in the case of single ionization. In the case of double ionization, significant discrepancies with theoretical predictions are found, indicating a breakdown of the independent-electron model. Furthermore, evidence is provided that dynamic correlation effects in the two-electron continuum strongly influence the angular distribution of ejected electrons for double ionization.

PACS numbers: 34.50.Fa, 34.50.Pi

Studies of ionization by charged particles are important not only to atomic physics, but also to plasma physics, astrophysics, thermonuclear fusion research, and ion implantation. Accurate cross sections are needed in these fields, but only single-electron processes are at present well understood. Multielectron processes are influenced by mean-field effects, e.g., dynamic screening, or different kinds of correlation processes. Thus, predictions of the independent-electron model (this model neglects the above-mentioned effects), on which most of the current theories are based, are questionable in the case of multielectron transitions.¹⁻⁴

One of the recently investigated correlation processes involving continuum electrons is the so-called two-electron Thomas peak, which appears as a structure in the (neutral) projectile-scattering cross section and in the angular distribution of ejected electrons.^{5,6} A breakdown of the independent-particle model (IPM) was found in a comparison of total proton and antiproton cross sections for single and double ionization of He.⁷ It was not clear until now whether the significant deviations between proton and antiproton data for double ionization are due to mean-field effects or due to dynamic correlation effects.⁸ Thus, it is interesting to investigate multiple-differential double-ionization cross sections, in order to get some new insights into the mechanisms responsible for double ionization. Electron spectroscopy,^{9,10} especially in connection with the measurement of the projectile-scattering angle¹¹ or the recoil-ion charge state,¹² is a sensitive tool for identifying excitation mechanisms, and for testing the limits of even sophisticated collision theories. In this work we go one step further and present absolute angular distributions of ejected electrons for proton-induced single and double ionization of He at a small impact parameter ($b=0.02$ a.u.). It will be shown that the independent-electron model is not able to predict the absolute double-ionization probability. Furthermore, evidence is provided that the angular distribution for double ionization is strongly influenced

by correlation effects.

Figure 1 displays the experimental setup for the measurement of triple coincidences. A Van de Graaff generator was used to produce a 300-keV beam, which was charge-state analyzed and collimated. Electrons emitted in $H^+ + He$ collisions were measured in coincidence with scattered ions as described in detail elsewhere.¹³ Scattered projectiles were detected with a fast position-sensitive particle detector and ejected electrons were detected with an electron time-of-flight analyzer. High coincidence rates with small random-coincidence rates were achieved due to the relatively large solid angle (130 msr) of the electron spectrometer as well as the fact that the time-of-flight analyzer analyzes all of the incoming electrons. In order to measure triple coincidences between projectiles, recoil ions, and electrons, we used a newly developed recoil-ion time-of-flight analyzer¹⁴ which keeps the target region nearly field free (< 1 V/cm) during the collision. About 200 ns after an electron is detected, a pulsed field of about 200 V/cm is applied to the target region. This field pushes the low-energy recoil ions into the recoil time-of-flight analyzer, where they are further accelerated depending on their

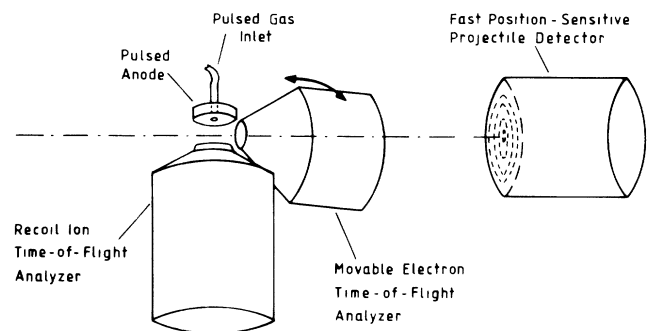


FIG. 1. Experimental setup for triple coincidences between electrons, recoil ions, and scattered projectiles.

charge state. The time difference between pulsing the target region and detecting the ion is a direct measure of the recoil-ion charge state.

In order to improve the accuracy of the data analysis and to check for random signals, the target gas flow was switched every 10 min between two gas inlets (directly above the target center and 30 cm away). This allows for the determination of the number of events, scattered projectiles as well as double and triple coincidences, occurring inside and outside the target region. The data analysis follows closely the description given in Ref. 13. In this paper we present doubly and singly differential electron emission probabilities, as a function of the final target charge state. It is noted that measured double-ionization yields are twice that of the double-ionization probabilities because of two electrons being ejected. Figure 2 displays typical electron spectra for singly and doubly charged recoil ions measured at an electron ejection angle of 40° and a projectile-scattering angle of 0.5° . It is seen from the figure that single ionization is about 2 orders of magnitude more probable than double ionization.

The theoretical formulation of multielectron processes is conveniently discussed in terms of the independent-particle model, as given by McGuire and Weaver.¹⁵ By neglecting mean-field effects and dynamic correlation effects, measurable quantities may be expressed on the basis of simple binomial statistics, and, if necessary, impact-parameter integration. As spin interactions are of no importance the two electrons are completely distinguishable throughout the collision. Therefore, there can be no effect due to statistical correlation (Pauli blocking).

The singly differential electron ejection probabilities $dP/d\Omega$ for single and double ionization ($q_i=1,2$) of

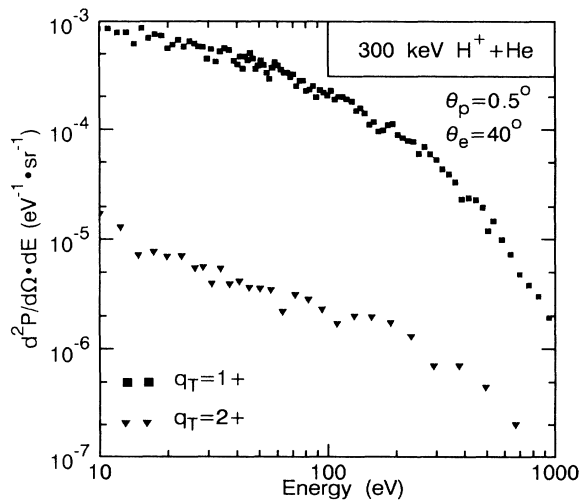


FIG. 2. Absolute doubly differential electron emission probabilities for a projectile-scattering angle of 0.5° in 300-keV $H^+ + He$ collisions for different final target charge states.

helium atoms may be written as

$$\frac{dP}{d\Omega_e}(q_i=1, \Theta_e, b) = 2 \frac{dI}{d\Omega_e}(\Theta_e, b) \left(1 - \int d\Omega'_e \frac{dI}{d\Omega_e}(\Theta'_e, b) \right) \quad (1)$$

and

$$\frac{dP}{d\Omega_e}(q_i=2, \Theta_e, b) = \frac{dI}{d\Omega_e}(\Theta_e, b) \int d\Omega'_e \frac{dI}{d\Omega_e}(\Theta'_e, b), \quad (2)$$

where $dI/d\Omega$ is the singly differential ionization probability for one active electron, as given by any IPM theory. It is emphasized that Eqs. (1) and (2) imply identical angular distributions of ejected electrons (except for a constant factor), independent of the degree of ionization. The projectile-scattering angle of $\Theta_p=0.5^\circ$, investigated in this work, corresponds to an impact parameter of $b=0.02$ a.u. This impact parameter is small enough compared to the mean orbital radius of the He ground state so that the $b-\Theta_p$ relation does not depend on the degree of ionization. This is not true for previous measurements of the total single and double ionization as a function of the projectile-scattering angle,^{4,16} as in those measurements the projectile deflection was dominated by the interaction between projectile nucleus and target electrons.¹⁷

Figure 3(a) displays the angular distribution of eject-

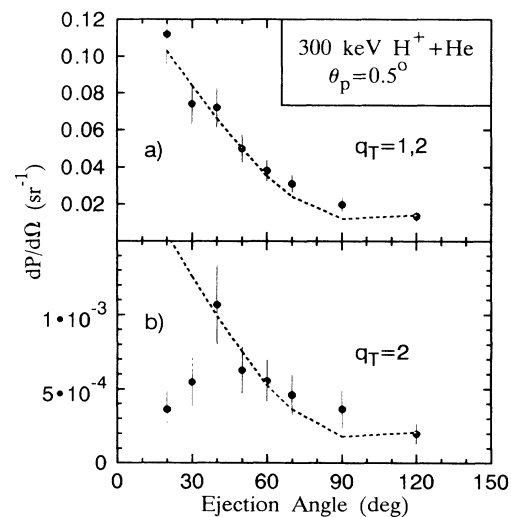


FIG. 3. Absolute singly differential electron emission probabilities for a projectile-scattering angle of 0.5° in 300-keV $H^+ + He$ collisions as a function of the electron ejection angle. The error bars represent an upper estimate of the overall error. (a) Gross ionization yields (single plus double ionization). Coupled-channel calculation, dashed line (Ref. 18). (b) Double ionization probabilities. Coupled-channel calculation (normalized to the experimental data for ejection angles $> 30^\circ$), dashed line (Ref. 18).

ed electrons for single plus double ionization measured in coincidence with a projectile at a scattering angle of 0.5° . The singly differential probabilities $dP/d\Omega$ were obtained from the integration of absolute doubly differential probabilities over energy. The angular distribution in Fig. 3(a) shows a pronounced increase towards small electron ejection angles. For comparison, results of a single-centered atomic-orbital (AO) coupled-channel calculation¹⁸ (5 bound states and 85 damped continuum wave packets for orbital angular momenta of $l=0$ to $l=8$ and angular-momentum-projection numbers $m=0$ and 1) are also displayed in Fig. 3(a). The model includes numerical nonhydrogenic single-electron wave functions and dynamic curved projectile trajectories. The main advantage of the AO model compared to the first-order perturbation theory¹⁷ is that an infinite number of interactions (instead of only one) between the projectile and an active target electron is taken into account. It is seen that there is good agreement between theory and experiment. It is emphasized that the theory is based on the independent-electron model. Thus, gross ionization probabilities ($q_i=1,2$) are well described within an independent-particle model for the electronic motion (see also Ref. 3).

Figure 3(b) displays the angular distribution of ejected electrons measured in coincidence with a *doubly* charged He ion and a projectile at a scattering angle of 0.5° . Less than 10% of those events correspond to transfer ionization. This was estimated with two-active-electron classical-trajectory Monte Carlo (CTMC) calculations,¹⁹ and additionally with previously measured data.⁵

The dashed line in Fig. 3(b) represents the same coupled-channel results as shown in Fig. 3(a), but is multiplied with a constant factor of 0.015. This factor corresponds to the total single-electron ionization probability [the integral in Eq. (2)] divided by 2 and was determined from a fit to the experimental double-ionization data for ejection angles $\geq 40^\circ$. As mentioned above, the angular distribution for single and double ionization should be identical. The striking difference in the angular distribution of ejected electrons at emission angles below 40° is the key point to this investigation and will be discussed in the last paragraphs. First, it should be noted that the total single-electron ionization probability of 0.03 as determined from the fit is in contradiction with the absolute ionization probability as determined from the angle integration of the coupled-channel results and the experimental data for single ionization. The total single-electron ionization probability obtained from this integration is 0.19. Thus, by accounting for nothing else than the experimental data and the IPM, we find two total ionization probabilities which differ by a factor of 6. This is a clear sign for a breakdown of the IPM in the case of double ionization.

Two effects seem to be responsible for this large

discrepancy. One is the initial-state correlation, as predicted by multiconfiguration Hartree-Fock codes, and corresponds to a reduction of the probability density for finding one electron near the other. This leads to a reduction of the two-electron density near the projectile path. Hence, the double-ionization probability will be reduced in comparison with IPM predictions.²⁰ However, another effect, namely, a mean-field effect, might dominate the reduction of the double-ionization probability. It was demonstrated in recent CTMC calculations¹⁹ that a dynamic target screening might lead to a reduction of the double-ionization probability by a factor of 2 to 4 in comparison with calculations using a static screened target potential. This reduction may be viewed as a binding effect: When the "first electron" is ionized, the "second electron" will interact with an unscreened nuclear potential. The enhanced attraction by the target nucleus will reduce the ionization probability for the second electron. It is emphasized that a relaxation of the second electron's density distribution, as considered in previous works,¹² is not necessary for this reduction.

Both effects discussed above are included in the forced impulse method (FIM) calculations by Ford and Reading²¹ where electron correlation is fully incorporated. It is emphasized that our total double-ionization probability of 0.005 ± 0.002 is in excellent agreement with the FIM results for small impact parameters. These results indicate that the proton-induced double-ionization amplitude is strongly reduced due to effects which go beyond the IPM, as discussed above. Furthermore, this reduction is in harmony with the findings of Andersen *et al.*,⁷ where the ratio of double to single ionization was about a factor of 2 lower for protons than the ratio for antiprotons.

The deviations between experimental data and the normalized coupled-channel results in Fig. 3(b) for electron ejection angles smaller than 40° are obviously inconsistent with any IPM prediction as given by Eqs. (1) and (2). The absolute experimental value for 20° is a factor of 35 lower than the corresponding value predicted by Eq. (2) for double ionization. Dynamic-screening CTMC calculations¹⁹ for the angular distributions in 300-keV $H^+ + He$ collisions do not show any significant redistribution effect for double ionization near 0° . As these calculations incorporate dynamic mean-field effects, we attribute the reduction of the double-ionization intensity at angles smaller than 40° to a correlation process due to the residual electron-electron interaction. The most likely process which could lead to a redistribution of the angular distribution is a repulsion between the two simultaneously ionized electrons. In the language of quantum mechanics this corresponds to dynamic-state configuration interaction (or dynamic correlation).

In the following, an estimate will be given to show that the proposed electron-electron repulsion is able to

significantly reduce the electron intensity near 0° . From our measured energy spectra we determined a mean energy of 124 eV for electron ejection below 50° . The mutual repulsion of two electrons may be estimated from the adiabatic distance, from the total ionization probability, or simply from the difference of the He ground-state energy and the corresponding hydrogenlike binding energy. Typical values for the interaction potential between both electrons are between 30 and 120 eV. The angular deflection, corresponding to the mean ejection energy and the electron-electron interaction energy, ranges from 15° to 30° for each of the two emitted electrons. A deflection smaller than the estimated value would not lead to any visible effect in Fig. 3(b), but much larger values would result in a constant electron intensity, independent of ejection angle. Furthermore, it is noted that the repulsion is considerably enhanced for low-energy electrons and should show the characteristics of the Wannier effect²² in the low-energy limit.

Because high-energy electrons are less deflected, the mean energy of ejected electrons should be enhanced in the case of double ionization at forward angles. This is in harmony with our measured doubly differential ionization probabilities. However, the mutual repulsion can lead not only to angular-momentum exchange between both electrons, but also to an exchange of energy, similar to the case of an Auger transition. One electron would gain energy and the other one would be thrown back into a bound state.

In summary, for the first time an angular distribution of ejected electrons is presented for double ionization in 300-keV $H^+ + He$ collisions. Good agreement is found between summed experimental data, single plus double ionization, and results of an atomic-orbital coupled-channel calculation. Comparison is made between experimental double-ionization results and predictions of the independent-particle model (IPM), without referring to additional model assumptions. In the case of double ionization, electron ejection in forward directions ($< 40^\circ$) is strongly suppressed compared to the IPM predictions. This is not only an indication for a breakdown of the IPM, it also is consistent with an electron-correlation mechanism in the two-electron continuum. Comparison with electron-electron-projectile coincidence measurements and with explicit calculations of correlated double ionization would be desirable for a more quantitative elucidation of the proposed redistribution mechanism.

The authors would like to thank U. Stettner for his help during several stages of the experiment.

^(a)On leave from the University of Lund, Lund, Sweden.

¹J. H. McGuire, Phys. Rev. Lett. **49**, 1153 (1982); Nucl. Instrum. Methods Phys. Res., Sect. B **10**, 18 (1985); Phys. Rev. A **36**, 1114 (1987).

²N. Stolterfoht, in *Proceedings of the Conference on the Spectroscopy and Collisions of Few Electron Ions*, Bucharest, edited by V. Florescu and V. Zoran (World Scientific, Singapore, 1989), pp. 342–394.

³J. F. Reading and A. L. Ford, Comments At. Mol. Phys. **23**, 301–309 (1990).

⁴E. Y. Kamber, C. L. Cocke, S. Cheng, and S. L. Varghese, Phys. Rev. Lett. **60**, 2026 (1988).

⁵R. Hippler, G. Schiwietz, and J. Bossler, Phys. Rev. A **35**, 485 (1987).

⁶J. Pálkás, R. Schuch, H. Cederquist, and O. Gustafsson, Phys. Rev. Lett. **63**, 2464–2467 (1989).

⁷L. H. Andersen, P. Hvelplund, H. Knudsen, S. P. Møller, K. Elsner, K. G. Rensfeld, and E. Uggerhøj, Phys. Rev. Lett. **57**, 2147 (1986); Phys. Rev. A **36**, 3612 (1987).

⁸Dynamic correlation (Refs. 1 and 2) is understood in this work as an effect on the residual electron-electron interaction during a collision.

⁹N. Stolterfoht, C. C. Havener, R. A. Phaneuf, J. K. Swenson, S. M. Shafroth, and F. W. Meyer, Phys. Rev. Lett. **57**, 74 (1986); N. Stolterfoht, D. Schneider, J. Tanis, H. Altevogt, A. Salin, P. D. Fainstein, R. Rivarola, J. P. Grandin, J. N. Scheurer, S. Andriamonje, D. Bertault, and J. F. Chemin, Europhys. Lett. **4**, 899 (1987); S. T. Manson, L. H. Toburen, D. H. Madison, and N. Stolterfoht, Phys. Rev. A **12**, 60 (1975).

¹⁰R. Mann and H. Schulte, Z. Phys. D **4**, 343 (1987).

¹¹G. Schiwietz, Phys. Rev. A **37**, 370–376 (1988); G. Schiwietz, B. Skogvall, N. Stolterfoht, D. Schneider, V. Montemayor, and H. Platten, Nucl. Instrum. Methods Phys. Res., Sect. B **40/41**, 178–183 (1989).

¹²R. Hippler, J. Bossler, and H. O. Lutz, J. Phys. B **17**, 2453 (1984).

¹³G. Schiwietz, B. Skogvall, J. Tanis, and D. Schneider, Phys. Rev. A **38**, 5552 (1988); G. Schiwietz, U. Stettner, T. Zouros, and N. Stolterfoht, Phys. Rev. A **35**, 598 (1987).

¹⁴G. Schiwietz, B. Skogvall, N. Stolterfoht, D. Schneider, and V. Montemayor, in *Proceedings of the Conference on the Physics of Electronic and Atomic Collisions*, edited by A. Dalgarno, R. S. Freund, P. M. Koch, M. S. Lubell, and T. B. Lucatorto, AIP Conference Proceedings No. 205 (American Institute of Physics, New York, 1990), pp. 299–308.

¹⁵J. H. McGuire and L. Weaver, Phys. Rev. A **16**, 41 (1977).

¹⁶J. P. Giese and E. Horsdal, Phys. Rev. Lett. **60**, 2018 (1988).

¹⁷A. Salin, J. Phys. B **22**, 3901–3914 (1989).

¹⁸G. Schiwietz, Phys. Rev. A **42**, 296–306 (1990).

¹⁹V. Montemayor and G. Schiwietz, Phys. Rev. A **40**, 6223–6230 (1989); G. Schiwietz and V. Montemayor (unpublished).

²⁰A. E. Wetmore and R. E. Olson, Phys. Rev. A **38**, 5563 (1988).

²¹A. L. Ford and J. R. Reading, J. Phys. B **23**, 2567–2578 (1990).

²²G. H. Wannier, Phys. Rev. **90**, 817 (1953).